Fuel 137 (2014) 277–284

Contents lists available at ScienceDirect

Fuel

journal homepage: www.elsevier.com/locate/fuel

Influence of pressure on the heat of biomass pyrolysis

Lucia Basile, Alessandro Tugnoli, Carlo Stramigioli, Valerio Cozzani *

LISES – Dipartimento di Ingegneria Civile, Chimica, Ambientale e dei Materiali, Alma Mater Studiorum Università di Bologna, via Terracini 28, 40131 Bologna, Italy

HIGHLIGHTS

- Effect of pressure on the heat requirements of biomass pyrolysis were investigated.
- An increase in the operating pressure reduces the heat requirements of the pyrolysis process.
- Heat of pyrolysis process may shift from endothermic to exothermic at higher pressures.
- The heat of reaction as a function of pressure was shown to fit a Langmuir adsorption curve.
- A strong correlation was found between the final char yield and the overall reaction heat.

ARTICLE INFO

Article history:
Received 4 April 2014
Received in revised form 3 July 2014
Accepted 24 July 2014
Available online 5 August 2014

Keywords:
Biomass
Pyrolysis
Thermal effects
High pressure
Differential scanning calorimetry

ABSTRACT

Pyrolysis may be a first step in biomass to biofuels conversion processes. The present study investigated the influence of pressure on the thermal effects associated to biomass pyrolysis. Four energy crops were selected for experimental characterization: corn stalks, poplar, switchgrass Alamo and switchgrass Trailblazer. The heat demand of the pyrolysis process was measured by differential scanning calorimetry at pressures ranging from 0.1 to 4 MPa, using a specifically developed experimental configuration. An increase of the operating pressure resulted in a lower heat demand and in an increase in the final char yield. The results obtained suggest the presence of a competitive mechanism between the endothermic reactions of the primary decomposition process, leading to the formation of volatiles, and the exothermic vapor–solid interactions, leading to secondary char formation.

1. Introduction

The continuous increase in the concentration of carbon dioxide in the atmosphere is calling for the exploitation of renewable and carbon–neutral energy sources [1]. As a consequence, important resources were dedicated world-wide to the development of processes for the recovery of energy from non-conventional fuels [2,3]. Biomass is expected to extend its role as a carbon–neutral energy source in the future energy scenarios, as a consequence of the adoption of policies aiming at fuel diversification and at the reduction of fossil fuel dependence [4]: e.g. European Union Directive 2009/28/EC [5–7] provides legally binding targets for the share of energy from renewable sources in the Member States for the year 2020.

Pyrolysis conversion processes are an important technological option for biofuel production and energy recovery from biomass and wastes [2,8,9]. Pyrolysis is also a first step in gasification and in other thermochemical conversion processes for the exploitation of energy from biomass [10,11]. Thus, the investigation of the influence of operating conditions on the outcomes of the thermal conversion of biomass feedstock in pyrolysis processes is an important element to enhance the design and the optimization of new biomass to energy processes.

High pressure reactors for biomass conversion may have several potential advantages, as higher yields of valuable products, higher throughput, lower compression costs of product gases, increased reaction rates [12,13]. However, the design of high pressure gasification and pyrolysis processes needs to gather detailed data on the effects of operating pressure on the product yields and on the thermal effects during biomass conversion.

Limited experimental data are available on the influence of pressure on the distribution of pyrolysis products and on the heat demand of the process. In 1983 Mok and Antal [12], using a tubular flow reactor embedded in a differential scanning calorimeter, report an increase in the yield of char from cellulose from 12% to 22% when the operating pressure is increased from 0.1 to 2.5 MPa. Blackadder and Rensfelt [13] report that char yield from

* Corresponding author. Tel.: +39 051 2090240; fax: +39 051 2090247.
E-mail address: valerio.cozzani@unibo.it (V. Cozzani).

http://dx.doi.org/10.1016/j.fuel.2014.07.071
0016-2361/

cellulose pyrolysis increases from 6% at 0.1 MPa to 15% at 4 MPa in a pressurized thermogravimetric analyzer (TG). The same authors report that the char yield from wood pyrolysis increased from 21% to 28% over the same pressure range. Richard and Antal [14] report an increase in the char yield from cellulose from 19% to 41% when pressure is increased from 0.1 to 2.0 MPa. In contrast, Kandiyoti and co-workers [15] report a limited influence of operating pressure on the char yields from Eucalyptus sawdust pyrolysis in a hot-rod reactor where the volatiles were quickly removed from the reaction zone.

Available data concerning the influence of operating pressure on the thermal effects of the pyrolysis process are even more limited. Mok and Antal [16] report that during the pyrolysis of cellulose the increase of the operating pressure reduces the required heat of reaction, increases the yield of char and of CO_2, and reduces the yields of CO and of all hydrocarbons formed in the process. Several other studies evidence a relation among secondary reactions of volatiles and the overall heat demand of the pyrolysis process even at atmospheric pressure [17–22].

The present study is focused on the influence of pressure on the heat of pyrolysis of four lignocellulosic biomass crops. Experimental runs were carried out using a high-pressure differential scanning calorimetry (DSC). A specific gas flow rate control system was developed to allow the use of constant purge gas flow conditions in experimental runs.

2. Experimental

2.1. Materials

Four biomass samples were used in experimental runs: corn stalks, poplar, switchgrass "Alamo" and switchgrass "Trailblazer". The biomass feedstock was provided by the Department of Agro-Environmental Science and Technology of the University of Bologna (Italy). The material was farmed and harvested in Ozzano and Cadriano (Bologna, Italy), dried overnight (15 h at 105 °C) and ground up to a particle size lower than 1 mm. Table 1 reports the proximate analysis of the biomass samples, both on "as received" and on dry basis.

Samples for TG and DSC runs were obtained pressing and punching the biomass particles to compact discs (about 5 mm diameter and 0.4–0.7 mm height depending on the desired sample weight) that fitted the crucibles used in DSC analysis.

2.2. Experimental techniques and procedures

Thermogravimetric (TG) experimental data at atmospheric pressure were obtained using a TA Instruments-Waters (USA) TGA-Q500 device. Samples used in TG runs were previously dried at 105 °C under a nitrogen flux of 60 ml/min for 10 min. Constant heating rate runs were carried out on the dry samples using a pure nitrogen purge gas flow rate of 60 ml/min, a heating rate of 10 °C/min and a final temperature of 950 °C. The purge gas was then switched to air (60 ml/min for 10 min) in order to allow detecting the ash content of the sample. The TG data reported in the following were calculated as the mean of at least 3 experimental runs. Differences in weight loss with respect to temperature in different runs were less than 2%.

Differential scanning calorimetry (DSC) data were obtained using a DSC-Q2000 for atmospheric runs and a DSC Q20P for runs under pressure. Both DSC devices were supplied by TA Instruments (USA). In the DSC-Q2000 atmospheric tests, typical sample weights between 3 and 13 mg and aluminum crucibles (d = 5.1 mm) were used. The sample cell was conditioned by a constant nitrogen purge flow (50 ml/min) at atmospheric pressure. Baseline calibration of the DSC signal was obtained by constant heating rate runs on the empty cell and on two 95 mg sapphire samples to determine the thermal resistance and heat capacity of the reference and sample sensor. Heat flow and temperature calibration were obtained by constant heating rate runs carried out on known standards (indium and lead). More details on the DSC calibration procedures are available in the literature [12,16].

Runs under pressure were carried out in the DSC-Q20P device using typical sample weights of about 8 mg. A specific gas circuit was built to allow DSC runs under pressure in the presence of a constant purge gas flow. Fig. 1 shows the experimental set-up. A control loop was realized to pressurize the test cell up to the selected operating pressure and to keep a constant pressure and a constant purge gas flow during the test. An EL-PRESS P-702CV pressure controller and an EL-FLOW F-201CV mass flow controller, both by Bronkhorst (The Netherlands) were used for pressure and gas flow control. The same procedures used for the DSC Q2000 were applied for baseline, heat flow and temperature calibration of the DSCQ 20P. Pressure calibration was based on the comparison of pressure values from the instrument with those from an external pressure gauge. Further details on DSC calibration procedures are reported in the literature [12,16].

In all experimental runs, the inlet nitrogen flow rate was fixed to 0.050 Nl/min, corresponding to an outlet flow rate of 50 ml/min, in order to obtain a constant heat capacity of the gas flow during experimental runs. Runs were carried out at the following operating pressures: 0.1, 0.5, 1, 2, and 4 MPa. Gas residence time in the DSC is affected by temperature and pressure, but was always comprised between about 0.1 and 0.9 s, well below the time scale of DSC measurements.

The DSC runs were performed using 5 mm diameter aluminum crucibles. The crucibles were used without lid to maximize mass transfer and ease the separation of volatiles from the solid substrate. Samples used in DSC runs were previously dried at 105 °C under a nitrogen flux of 60 ml/min for 10 min. All DSC runs were started at 105 °C. A constant heating rate of 10 °C/min, was used up to the final temperature, set at 550 °C. At the end of each run, the furnace was cooled down to 30 °C under nitrogen purge gas flow and a second run was performed on the char sample using the same temperature–time program. At the end of the DSC runs the char residue was weighed, and the yields in char and volatile products were estimated. The set-up of the DSC devices used for experimental runs do not allow the separate determination of the yields in gaseous and liquid products among volatile species. It should also be remarked that the heating rates allowable in TG

Table 1
Proximate analysis of the biomass samples used in the present study.

Biomass	wt% Dry basis			wt% As received			
	Volatile matter	Fixed carbon	Ash	Moisture	Volatile matter	Fixed carbon	Ash
Corn stalks	77.7	16.0	6.3	3.3	75.2	15.4	6.1
Poplar	81.8	14.8	3.4	2.2	80.0	14.4	3.3
Switchgrass "Alamo"	79.3	12.1	6.7	3.0	77.0	11.8	8.3
Switchgrass "Trailblazer"	64.1	8.6	27.3	3.4	61.9	8.3	26.4

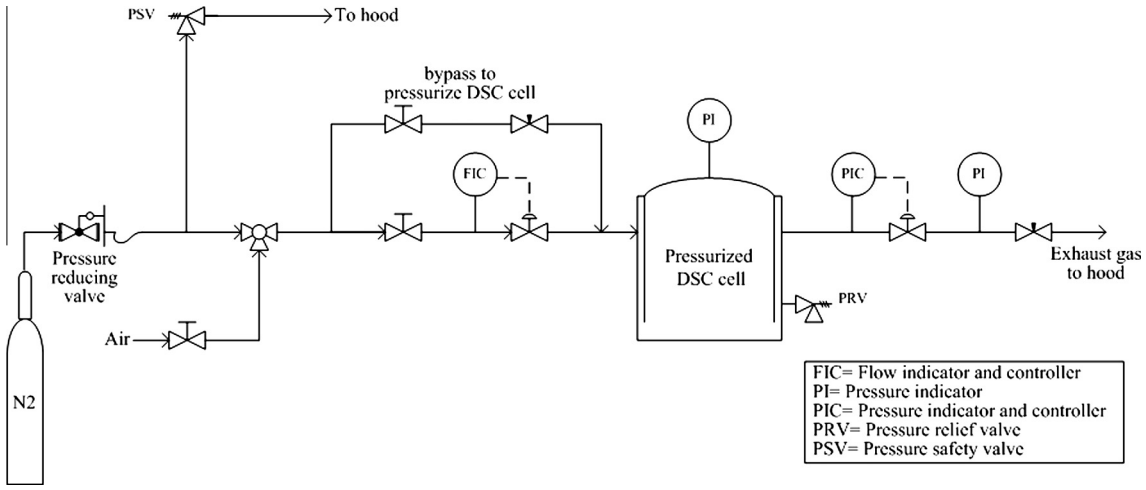

Fig. 1. Simplified scheme of the experimental set up used for DSC runs under pressure.

and DSC devices, used in the present study, only allow the reproduction of slow pyrolysis conditions.

3. Results and discussions

A preliminary characterization of the pyrolysis behavior of the four biomass crops selected in the present study was carried out at atmospheric pressure. Fig. 2 reports the weight loss (TG), the differential weight loss (dTG) and the raw heat flow curves from DSC experiments obtained using a pure nitrogen purge flow and a constant heating rate of 10 °C/min. As expected, Fig. 2 evidences that the main peaks of the dTG and DSC curves are almost at the same temperature and that thermal effects of the pyrolysis process at atmospheric pressure are endothermic, except those from corn stalks. Table 2 summarizes the char yields and the characteristic temperatures of the pyrolysis process identified for the four biomass samples. Char yield is defined as:

$$\eta_{daf} = \frac{m_{char} - m_{ash}}{m_0 - m_{ash}} \quad (1)$$

where m_0 is the initial sample weight (after drying at 110 °C), m_{char} is the final weight of the sample at the end of the constant heating rate ramp in nitrogen (550 °C), and m_{ash} is the weight of ashes as detected at the end of TG runs (950 °C). As evident from Fig. 2 and Table 2, corn stalks also evidence the highest char yield and lowest pyrolysis temperatures. On the other hand, poplar and

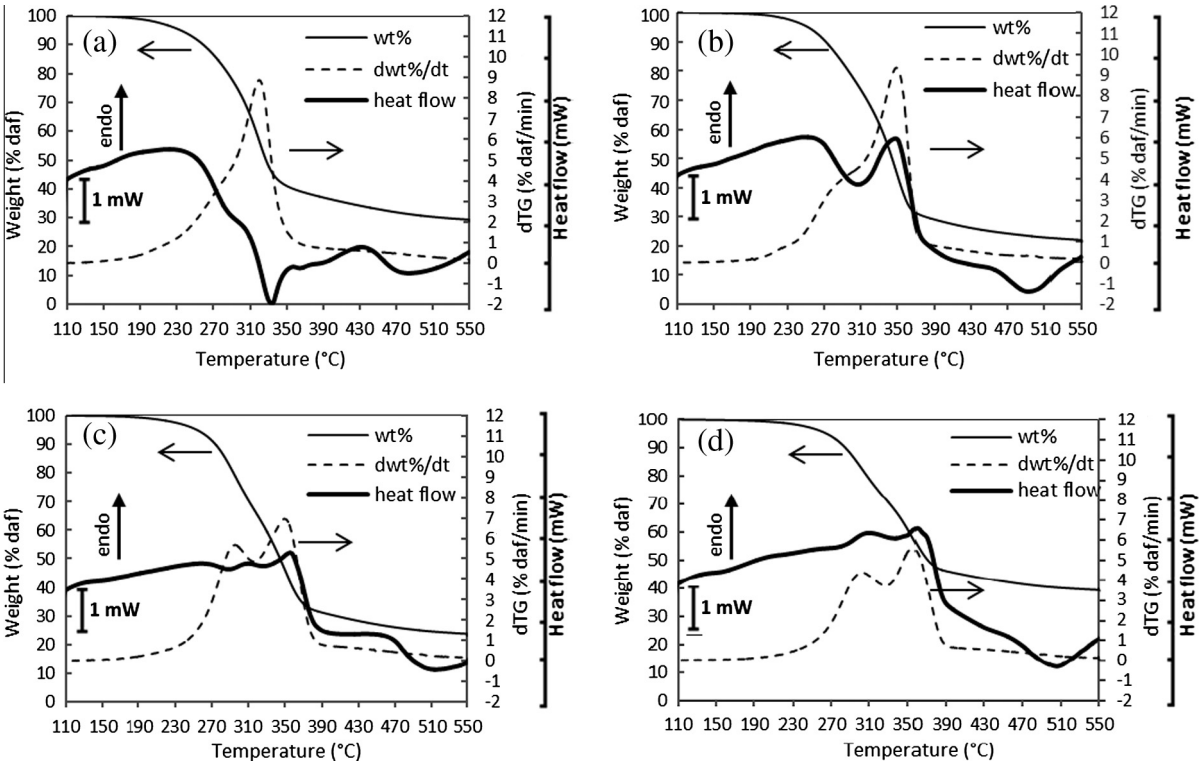

Fig. 2. TG, dTG and DSC results at atmospheric pressure for corn stalks (a), poplar (b), switchgrass "Alamo" (c) and switchgrass "Trailblazer" (d). Initial sample weight of about 8 mg was used in all experimental runs.

Table 2
Char yield, maximum decomposition rate and temperature at maximum decomposition rate for the pyrolysis at atmospheric pressure of the four biomass crops considered (initial sample weight of about 8 mg).

Biomass	Char yield up to 550 °C (% daf)	Maximum decomposition rate (wt% daf/min)	Temperature at maximum decomposition rate (°C)
Corn stalks	23.8	8.89	320
Poplar	19.8	9.36	349
Switchgrass "Alamo"	17.6	6.96	349
Switchgrass "Trailblazer"	11.5	5.59	355

switchgrass Alamo yield similar quantities of char and show the same temperature for the main peak in the dTG curve.

The influence of pressure on the thermal effects of the pyrolysis process was then analyzed, carrying out experimental runs at 0.5, 1, 2 and 4 MPa. Fig. 3 reports an example of the raw results obtained for poplar (10 °C/min constant heating rate, pure nitrogen purge gas flow). The figure clearly evidences a modification in the DSC curve as the operating pressure is increased.

In order to assess the influence of pressure on the thermal effects, it is necessary to obtain quantitative data for the heat of pyrolysis from the raw DSC curves reported in Figs. 2 and 3. In particular, it is necessary to separate the contribution of the pyrolysis reaction process from other thermal effects recorded by the DSC device. Actually the experimental curves obtained in a DSC analysis result from several contributions, some depending on the thermal behavior of the sample (heat capacity of the sample, latent heat of evaporation of volatile components, heat of primary pyrolysis, heat of secondary reactions) and some due to the experimental setup (asymmetric radiative heat exchange between the sample and the DSC cell due to the change in the surface emissivity of the biomass) [23]. The approach of Rath et al. [17], briefly summarized in the following, was used to obtain quantitative data for the heat of reaction from the DSC curves.

The effect of heat capacity of the sample (Q_{sh}) can be isolated by calculating a theoretical heat flow curve for sample heating from the data on the specific heat of biomass and char available in the literature [24–26]:

$$Q_{sh} = (1 - X(T)) \cdot m_0 C_{p,bio} \frac{dT}{dt} + X(T) \cdot m_{char} C_{p,char} \frac{dT}{dt} \quad (2)$$

where m_0 and $C_{p,bio}$ are respectively the initial sample weight and heat capacity, m_{char} and $C_{p,char}$ are respectively the final weight and heat capacity of the final solid residue (called "char" in the following discussion), T is the temperature, and $X(T)$ is a dimensionless sample conversion defined as:

$$X(T) = \frac{m_0 - m_T}{m_0 - m_{char}} \quad (3)$$

where m_T is the sample weight at temperature T. The values of $c_{p,bio}$ and $c_{p,char}$ can be experimentally measured or derived from generic correlations. In the present study the correlations proposed by Koufopanos et al. [27] were used in the calculations. The contribution of asymmetric radiative heat exchange was evaluated from the DSC run. Since the experimental heat flow of the second run carried out on char (Q_{char}) can be considered the sum of the sensible heat of the char and of the asymmetric radiative heat exchange [17], it is possible to calculate the radiative heat flow (Q_{rad}) as the difference between the experimental DSC curve obtained from the char after the pyrolysis run (see Section 2) and the heat flow needed to heat the char, calculated on the basis of char specific heat [23].

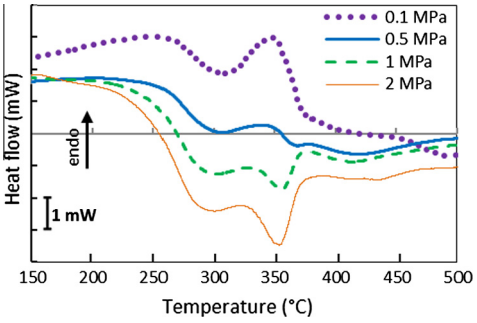

Fig. 3. DSC raw data for poplar, 10 °C/min, nitrogen purge gas, initial sample weight of 8 mg.

The heat flow due to the pyrolysis process (Q_r) may thus be obtained subtracting the radiation effect (Q_{rad}) and the contribution of heat capacity (Q_{sh}) from the experimental heat flow curve recorded for the biomass sample (Q_{exp}):

$$Q_r = Q_{\exp} - Q_{rad.} - Q_{sh} \quad (4)$$

The total heat requirement associated to the pyrolysis process is then calculated by numerical integration as:

$$H_p = \frac{1}{m_0} \int_{T_i}^{T_f} Q_r dT \quad (5)$$

where T_i and T_f are the initial and final temperatures of the decomposition process. The values of these temperatures depend on the biomass type and were evaluated from the dTG curve as the endpoints of the temperature interval for which the dTG value equals −0.5%/min. Reproducibility of heat flow data obtained by this procedure evidenced that maximum error in the final heat flow values was always lower than 10%.

Fig. 4 compares the curves obtained for the reaction heat (Q_r) at different operating pressures. As evident from the figure, the temperature range of the pyrolysis process and the peak temperature in the heat flow during the pyrolysis process are not dependent on pressure. This result suggests that when open DSC crucibles are used, as in the present study, the pyrolysis kinetics is not enhanced as when closed crucibles are used, confirming the findings of Mok et al. [28–30].

Nevertheless, Fig. 4 confirms that pressure has a strong influence on the thermal effects of the pyrolysis process for all the four biomass samples considered. As shown in Table 3, increasing the pressure a clear decrease in the heat demand of the pyrolysis process can be observed for all the materials. When increasing the pressure from 0.1 MPa to 4 MPa, the total heat of pyrolysis shifts from −50 J/g to −272 J/g for corn stalks, from 29 J/g to −283 J/g for poplar, from 37 J/g to −199 J/g for switchgrass Alamo, and from 92 J/g to −210 J/g for switchgrass trailblazer (negative values are used for exothermic processes). In the case of switchgrass Trailblazer, the change is so significant that a shift from an overall endothermic to an overall exothermic process takes place. In the case of corn stalks, the pyrolysis process is exothermic even at atmospheric pressure, but the results in Fig. 4 show that the heat generation in the process increases as well.

For the sake of clarity it should be remarked that the different heat demand of the pyrolysis process for different biomass species, ranging from exothermic to endothermic at atmospheric pressure, was previously reported in the literature (e.g. see the studies of Stenseng et al. [31], Strezov et al. [32], and Di Blasi et al. [33]).

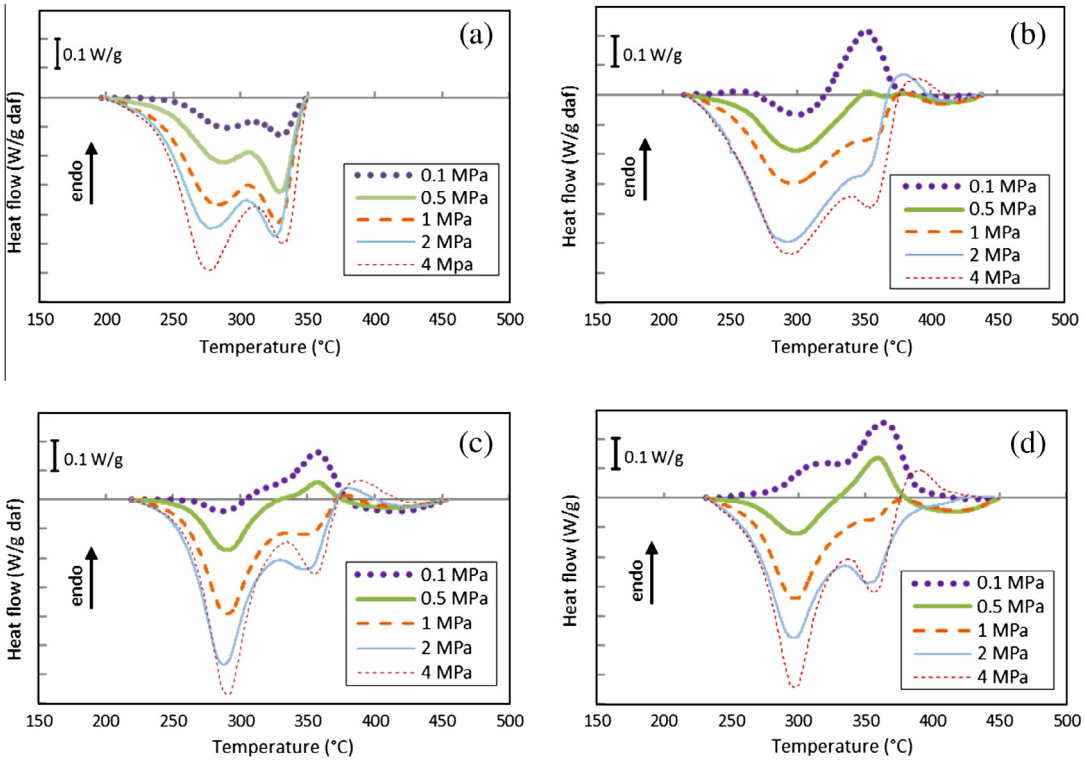

Fig. 4. Heat flow due to the pyrolysis process (Q_r) at different pressure for corn stalks (a), poplar (b), switchgrass Alamo (c) and switchgrass Trailblazer (d). Conditions: Pure nitrogen, 10 °C/min, crucibles without lids.

Table 3
Overall heat demand of the pyrolysis process obtained for the four biomass samples considered at different operating pressures (initial sample weight of about 8 mg). Negative values of the heat requirement correspond to an exothermic behavior.

Biomass	Pressure (bar)	Char yield (% daf)	Heat requirement, H_p (J/g ash-free mass)
Corn stalks	40	28.4	−272
Corn stalks	20	28.5	−229
Corn stalks	10	27.5	−171
Corn stalks	5	26.3	−118
Corn stalks	1	23.8	−50
Poplar	40	30.7	−283
Poplar	20	28.2	−272
Poplar	10	26.0	−191
Poplar	5	22.1	−71
Poplar	1	17.3	29
Switchgrass Alamo	40	27.3	−199
Switchgrass Alamo	20	26.4	−203
Switchgrass Alamo	10	23.2	−134
Switchgrass Alamo	5	21.4	−40
Switchgrass Alamo	1	15.1	37
Switchgrass Trailblazer	40	28.5	−210
Switchgrass Trailblazer	20	29.2	−212
Switchgrass Trailblazer	10	26.3	−123
Switchgrass Trailblazer	5	21.8	−21
Switchgrass Trailblazer	1	19.1	92

The differences were attributed to the different chemical composition of the biomass species, and in particular to their different content in extractives, hemicellulose and lignin [22,34–38].

The pressure has a strong influence also on the yields of char, as evident from the data in Table 3 reporting the overall heat of reaction from the pressurized DSC tests and the residual char yield. Increasing the operating pressure an evident increase in the total yield of char can be observed. The char yield increases from 24% to 28% for corn stalks, from 17% to 31% for poplar, from 15% to 27% for switchgrass Alamo and from 19% to 29% for switchgrass trailblazer. These results confirm the findings of Mok and Antal [12,16], that report that increasing the pressure from 0.1 to 2.5 MPa causes the pyrolysis process of biomass to shift from endothermic (heat requirement of about 230 J/g) to exothermic (heat generation of about −130 J/g), with char yield increasing from 12% to 22%.

The influence of pressure on the heat requirement of the pyrolysis process can be explained by the inhibition of the evaporation processes of high molecular weight products formed in the primary pyrolysis process, and, as a consequence, by the promotion of exothermic secondary reactions of the primary pyrolysis products. Exothermic secondary reactions of tar vapors, both homogeneous and heterogeneous, include processes such as cracking, partial oxidation, re-polymerization and condensation [16,22,27,34,38–44]. A detailed discussion of such reaction processes is out of the scope of the present study. Further details are provided in several literature publications, e.g. in the comprehensive studies of Ranzi et al. [45], Di Blasi [34,39], and Ahuja et al. [19].

The influence of operating conditions on the heat of pyrolysis recorded at atmospheric pressure was reported in previous studies, and was attributed to the influence of transport phenomena affecting the residence time of volatiles in the solid substrate [19,22,34,46–48]. Several studies suggest that while the primary pyrolysis process is endothermic, secondary reactions of volatiles may be highly exothermic [17,18,20,31,49,50]. Actually, higher pressures limit mass transfer, thus providing a higher residence time in the porous solid substrate of the volatile products from primary thermal degradation reactions. The highly reactive tarry vapors at high pressure have lower specific volumes. Consequently, their intra-particle residence time is prolonged. Thus, the partial pressure of the tarry vapor is higher, increasing the rate of the secondary exothermic decomposition reactions [51]. These effects can

be emphasized when the flow of gas through the particle bed is small, as is the case at high pressure [12,16,51]. Furthermore, the formation of secondary carbon from the tarry vapor is catalyzed by the charcoal [52,53]. Molecular diffusivities are also affected by increasing pressure and can limit the outflow of the tarry vapor from the solid particle [54].

In Fig. 5 the values calculated for the total heat of pyrolysis were plotted as a function of the operating pressure. As shown in the figure, the heat of pyrolysis decreases as the pressure increases, with an almost linear slope between 0.1 and 1 MPa. However, a plateau appears at pressures higher than 1 MPa. Although a number of factors may justify the results obtained, it is interesting to notice that such behavior may be in accordance with a Langmuir adsorption model of the volatiles, suggesting that adsorption equilibria may play a role in the immobilization of the volatile compounds responsible of the secondary reactions.

Assuming, for the sake of simplicity, that volatiles generated in the primary pyrolysis process may be considered as a single pseudocomponent, a phenomenological description of the immobilization of the volatiles in the solid can be most simply obtained by a Langmuir adsorption model. The Langmuir isotherm relates the adsorption of molecules on a solid surface to the pressure of the absorbed gas at a fixed temperature:

$$\vartheta_v = \frac{\alpha p_v}{1 + \alpha p_v} \tag{6}$$

where θ_v is the fraction of volatile products adsorbed on the surface of the solid, p_v is the partial pressure of the adsorbate (the volatile pseudocomponent) in the gas phase and α is the Langmuir adsorption constant.

Several literature results allow assuming that the measured heat of reaction can be considered as the sum of two contributions, one due to the heat required for the primary degradation of the biomass (endothermic) and a second due to the secondary reactions of volatiles (exothermic) [17,18,20,31,49,50]. If secondary reactions of volatiles are assumed to be dependent on the fraction of volatile matter in the solid, the total heat of reaction can be expressed as:

$$H_P = H_1 + H_2 \bar{\vartheta}_v \tag{7}$$

where H_1 is the heat due to the primary degradation of biomass and H_2 is the heat due to the secondary reactions of volatiles, both assumed as independent on pressure, and $\bar{\vartheta}_v$ is the overall amount of pseudo-component available for the secondary reaction. Assuming that the contribution over the entire degradation range of a dynamic adsorption–desorption equilibrium between the vapor-phase and the surface of the solid can be still described by a correlation similar to Eqs. (6) and (7) can be written as:

$$H_P = H_1 + H_2 \frac{\alpha y_v P}{1 + \alpha y_v P} \tag{8}$$

where y_v is the molar fraction of the volatile pseudocomponent, and P is the total pressure of the system. The values of H_1, H_2 and the product αy_v are averaged values for the overall degradation, which were calculated by experimental data fitting. The best-fit parameters calculated from experimental runs are reported in Table 4, while Fig. 5 shows the results obtained applying Eq. (8) to calculate the heat of pyrolysis using the best-fit parameters of Table 4. The

Table 4
Best-fit parameters for Eq. (8) calculated from experimental runs.

Biomass	H_1	H_2	αy_i
Corn stalks	−23	−338	0.777
Poplar	68	−442	0.976
Switchgrass "Alamo"	89	−352	1.70
Switchgrass "Trailblazer"	147	−482	1.27

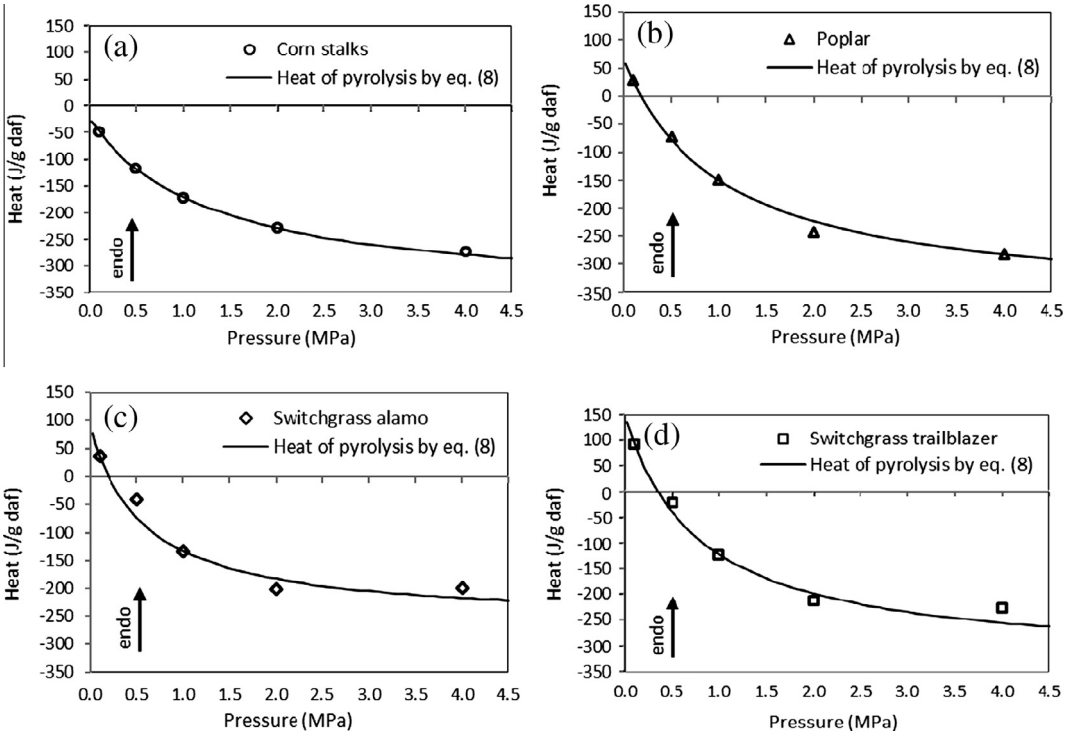

Fig. 5. Dependency of heat of reaction from the pressure for corn stalks (a), poplar (b), switchgrass Alamo (c) and switchgrass Trailblazer (d). Conditions: Pure nitrogen, 10 °C/min, crucibles without lids. Heat of pyrolysis curves were calculated by Eq. (8) using the best-fit parameters reported in Table 4.

figure shows that Eq. (8) provides a reasonable fitting of the trend recorded for the heat of pyrolysis with respect to operating pressure. Moreover, the presence of the plateau at higher operating pressures also seems to find a justification, since at higher pressures the number of molecules adsorbed increase to the point at which further adsorption is hindered by lack of space on the adsorbent surface. Clearly enough, the simplified model presented here supports only a phenomenological interpretation of the effect of pressure on the material degradation, and is not introduced to provide a detailed description of the complex mechanism underlying secondary char formation [19,22,48,51,54]. Nevertheless, the important role of secondary gas–solid interactions on the overall heat demand of the pyrolysis process seems to be confirmed by the above findings. The total heat of reaction changes with the pressure as described by the adsorption model. This supports the hypothesis that total heat of pyrolysis is influenced by the secondary reactions occurring between the volatiles adsorbed and the primary char.

In order to verify the strong correlation between char yield and heat of pyrolysis, an additional set of experimental DSC runs was carried out at atmospheric pressure, varying the initial weight of the sample in the range between 3 and 13 mg. The effect of the initial sample mass on secondary reactions has been a focal point of recent studies [55,56]. Clearly enough, the initial sample mass may affect the mass transfer process, increasing the residence time of volatiles in the solid substrate and enhancing secondary reactions. Fig. 6 shows the data obtained for the heat requirement of the pyrolysis process plotted with respect to the final char yield measured at the end of the DSC run. The figure evidences that a very similar trend to that obtained for experimental runs at different pressures is obtained. The trend is in agreement with previous results reported by Mok et al. [16] and by Antal and Grønli [51]. These findings further support the assumption that exothermic interactions among primary volatiles and residual solid leading to secondary char formation can strongly influence the overall thermal effects of the pyrolysis process, as observed in previous studies [16,18].

It is interesting to compare the results reported in Fig. 6 on biomass samples to those obtained by Mok et al. [16], that explored the effect of pressure on the heat demand of the pyrolysis process of cellulose samples. Fig. 7 reports a comparison of the overall heat demand with respect to char yield obtained in the present study for biomass samples and by Mok et al. [16] for cellulose. As shown in the figure, a very similar trend is found for the heat demand with respect to the char yield. However an evident offset is present, and the overall values of the heat demand at a given char yield seem to be lower for pure cellulose with respect to those of the biomass samples considered in the present study. Although the differences may origin from the different experimental conditions adopted, the results confirm that the presence of lignin may highly influence the char yield and the heat demand of the primary pyrolysis, as reported in several previous publications [34–38].

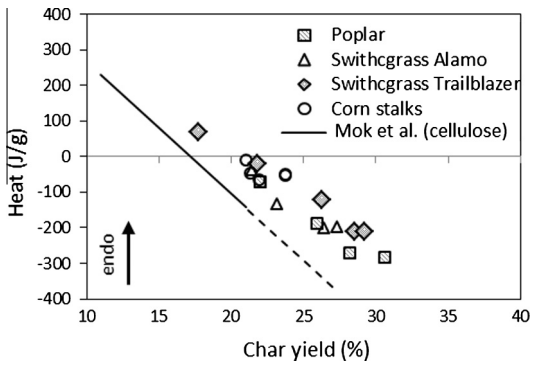

Fig. 7. Comparison of the results obtained for the heat demand of the pyrolysis process of cellulose [16] with those obtained in the present study.

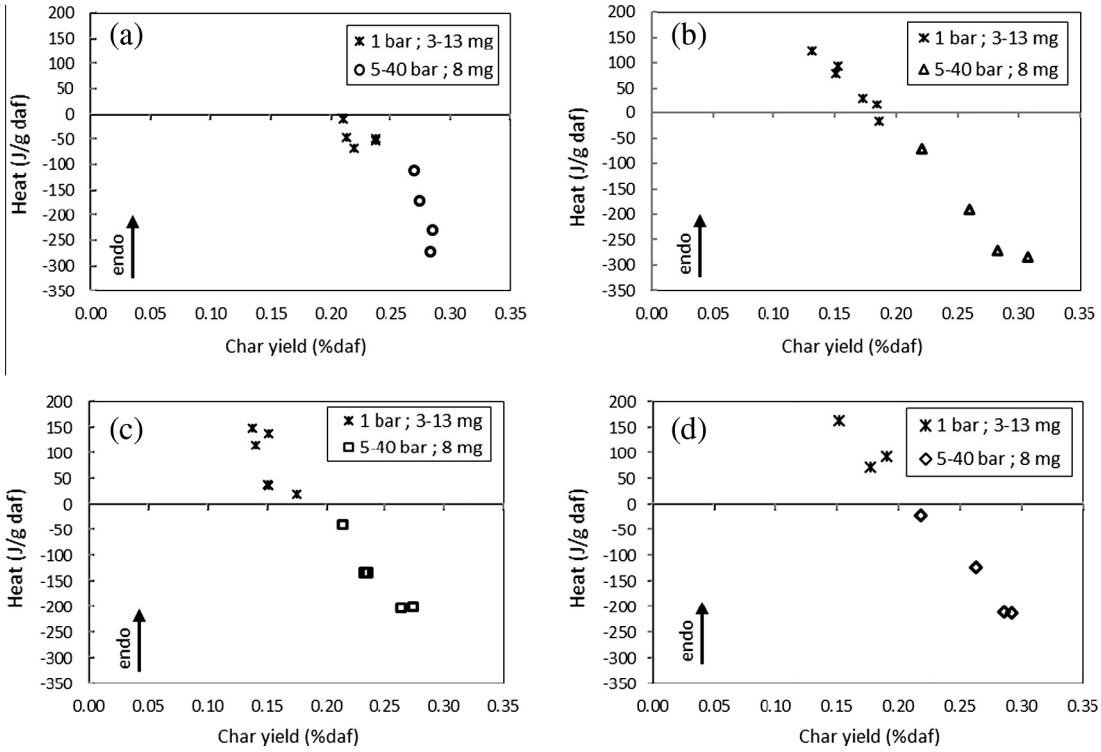

Fig. 6. Correlation of heat of reaction with final char yield for different operating pressures and different initial sample weight for corn stalks (a), poplar (b), switchgrass Alamo (c) and switchgrass Trailblazer (d). Conditions: Pure nitrogen, 10 °C/min, crucibles without lids.

4. Conclusions

The thermal effects of the pyrolysis process were investigated for four energy crops. The results evidence that an increase in the operating pressure reduces the heat requirements of the pyrolysis process, and the heat of pyrolysis reactions may shift from endothermic to exothermic. The heat of reaction as a function of pressure was shown to fit a Langmuir adsorption curve. The results suggest that the role of exothermic secondary reactions and the inhibition of the evaporation of high molecular weight compounds formed in the primary pyrolysis process may be among the main factors affecting the heat demand of the overall pyrolysis process. To confirm this assumption, a strong correlation was found between the final char yield and the overall reaction heat. The results obtained represent a further element towards the thorough understanding of biomass pyrolysis processes, that are a key-step in the thermal conversion of biomass substrates.

References

[1] McKendry P. Energy production from biomass (Part 1): Overview of biomass. Bioresour Technol 2002;83:37–46.
[2] Senneca O, Chirone R, Masi S, Salatino P. A thermogravimetric study of non fossil solid fuels. 1. Inert pyrolysis. Energy Fuels 2002;16:653–60.
[3] Bentsen NC, Jack MW, Felby C, Jellesmark Thorsen B. Allocation of biomass resources for minimising energy system greenhouse gas emissions. Energy 2014;69:506–15.
[4] Karampinis E, Vamvuka D, Sfakiotakis S, Grammelis P, Itskos G, Kakaras E. Comparative studies of combustion properties of five energy crops and greek lignite. Energy Fuels 2011;26:869–78.
[5] Directive 2009/28/EC of the European Parliament and of the Council of 23 April 2009 on the promotion of the use of energy from renewable sources and amending and subsequently repealing Directives 2001/77/EC and 2003/30/EC. OJ L 140, 5.6.2009; 2009. p. 16.
[6] European Commission Energy 2020 a strategy for competitive, sustainable and secure energy European Commission, Brussels, BE; 2010.
[7] Bishopa JDK, Axonb CJ, Trana M, Bonillac D, Banister D, McCullochd MD. Identifying the fuels and energy conversion technologies necessary to meet European passenger car emissions legislation to 2020. Fuel 2012;99:88–105.
[8] Bridgwater AV. Renewable fuels and chemicals by thermal processing of biomass. Chem Eng J 2003;91:87–102.
[9] Haydary J, Jelemensky L, Gasparovic L, Markos J. Influence of particle size and kinetic parameters on tire pyrolysis. J Anal Appl Pyrol 2012;97:73–9.
[10] McKendry P. Energy production from biomass (Part 2): Conversion technologies. Bioresour Technol 2002;83:47–54.
[11] Higman C, Van der Burgt M. Gasification. Elsevier Science; 2003.
[12] Mok Jr WSL, Antal MJ. Effects of pressure on biomass pyrolysis. I. Cellulose pyrolysis products. Thermochim Acta 1983;68:155–64.
[13] Blackadder W, Rensfelt EA. Pressurized thermo balance for pyrolysis and gasification studies of biomass wood and peat. Fundament Thermochem Biomass Convers 1985;747.
[14] Richard JR, Antal MJ. Thermogravimetric studies of charcoal formation from cellulose at elevated pressures. Adv Thermochem Biomass Convers 1994;784.
[15] Pindoria RV, Megaritis A, Messenbock RC, Dugwell DR, Kandiyoti R. Comparison of the pyrolysis and gasification of biomass: effect of reacting gas atmosphere and pressure on Eucalyptus wood. Fuel 1998;77:1247–51.
[16] Mok Jr WSL, Antal MJ. Effects of pressure on biomass pyrolysis. II. Heats of reaction of cellulose pyrolysis. Thermochim Acta 1983;68:165–86.
[17] Rath J, Wolfinger M, Steiner G, Krammer G, Barontini F, Cozzani V. Heat of wood pyrolysis. Fuel 2002;82:81–91.
[18] Gomez C, Velo E, Barontini F, Cozzani V. Influence of secondary reactions on the heat of pyrolysis of biomass. Ind Eng Chem Res 2009;48:10222–33.
[19] Ahuja P, Kumar S, Singh PC. A model for primary and heterogeneous secondary reactions of wood pyrolysis. Chem Eng Technol 1996;19:272–82.
[20] Milosavljevic I, Oja V, Suuberg EM. Thermal effects in cellulose pyrolysis: relationship to char formation processes. Ind Eng Chem Res 1996;35:653–62.
[21] Van de Velden M, Baeyens J, Brems A, Janssens B, Dewil R. Fundamentals, kinetics and endothermicity of the biomass pyrolysis reaction. Renew Energy 2010;35:232–42.
[22] Roberts AF. The heat of reaction during the pyrolysis of wood. Combust Flame 1971;17:79–86.
[23] Wolfinger MG, Rath J, Krammer G, Barontini F, Cozzani V. Influence of the emissivity of the sample on differential scanning calorimetry measurements. Thermochim Acta 2001;372:11–8.
[24] Babu BV, Chaurasia AS. Heat transfer and kinetics in the pyrolysis of shrinking biomass particle. Chem Eng Sci 2004;59:1999–2012.
[25] Gupta M, Yanga J, Roy C. Specific heat and thermal conductivity of softwood bark and softwood char particles. Fuel 2003;82:919–27.
[26] Kaletunc G. Prediction of specific heat of cereal flours: a quantitative empirical correlation. J Food Eng 2007;82:589–94.
[27] Koufopanos CA, Papayannakos N, Maschio G, Lucchesi A. Modelling of the pyrolysis of biomass particles. Studies on kinetics, thermal and heat transfer effects. Can J Chem Eng 1991;69:907–15.
[28] Mok WSL, Antal MJ, Szabo P, Varhegyi G, Zelei B. Formation of charcoal from biomass in a sealed reactor. Ind Eng Chem Res 1992;31:1162–6.
[29] Violette M. Memoire sur les Charbons de Bois. Ann Chim Phys 1853;32:304.
[30] Violette M. Memoire sur les Charbons de Bois. Ann Chim Phys 1855;39:291.
[31] Stenseng M, Jensen A, Dam-Johansen K. Investigation of biomass pyrolysis by thermogravimetric analysis and differential scanning calorimetry. J Anal Appl Pyrol 2001;765:58–9.
[32] Strezov V, Moghtaderi B, Lucas JA. Computational calorimetric investigation of the reactions during thermal conversion of wood biomass. Biomass Bioenergy 2004;27:459–65.
[33] Di Blasi C, Branca C, Sarnataro FE, Gallo A. Thermal runaway in the pyrolysis of some lignocellulosic biomasses. Energy Fuels 2014;28:2684–96.
[34] Di Blasi C. Modeling chemical and physical processes of wood and biomass pyrolysis. Prog Energy Combust 2008;34:47–90.
[35] Bilbao R, Mastral JF, Ceamanos J, Aldea ME. Modeling of the pyrolysis of wet wood. J Anal Appl Pyrol 1996;36:81–97.
[36] Di Blasi C, Branca C, Santoro A, Hernandez EG. Pyrolytic behavior and products of some wood varieties. Combust Flame 2001;124:165–77.
[37] Yang H, Yan R, Chen H, Lee DH, Zheng C. Characteristics of hemicellulose, cellulose and lignin pyrolysis. Fuel 2007;86:1781–8.
[38] Di Blasi C, Branca C, Masotta F, De Biase E. Experimental analysis of reaction heat effects during beech wood pyrolysis. Energy Fuels 2013;27:2665–74.
[39] Di Blasi C. Modeling intra- and extra-particle processes of wood fast pyrolysis. AIChE J 2002;48(10):2386–97.
[40] Bennadji H, Smith K, Shabangu S, Fisher EM. Low-temperature pyrolysis of woody biomass in the thermally thick regime. Energy Fuels 2013;27:1453–9.
[41] Pereza M, Grandaa M, Santamaria R, Morganb T, Menendeza R. A thermoanalytical study of the co-pyrolysis of coal-tar pitch and petroleum pitch. Fuel 2004;83:1257–65.
[42] Morf P, Hasler P, Nussbaumer T. Mechanism and kinetics of homogeneous secondary reactions of tar from continuous pyrolysis of wood chips. Fuel 2002;81:843–53.
[43] Bradbury AGW, Sakai Y, Shafizadeh F. Kinetic model for pyrolysis of cellulose. J Appl Polym Sci 1979;23:3271–80.
[44] Branca C, Di Blasi C, Elefante R. Devolatilization and heterogeneous combustion of wood fast pyrolysis oils. Ind Eng Chem Res 2005;44:799–810.
[45] Ranzi E, Cuoci A, Faravelli T, Frassoldati A, Migliavacca G, Pierucci S, et al. Chemical kinetics of biomass pyrolysis. Energy Fuels 2008;22:4292–300.
[46] Curtis LJ, Miller DJ. Transport model with radiative heat transfer for rapid cellulose pyrolysis. Ind Eng Chem Res 1988;27:1775–83.
[47] Williams PT, Besler S. The influence of temperature and heating rate on the slow pyrolysis of biomass. Renew Energy 1996;7:233–50.
[48] Seebauer V, Petek J, Staudinger G. Effects of particle size, heating rate and pressure on measurement of pyrolysis kinetics by thermogravimetric analysis. Fuel 1997;76:1277–82.
[49] Roberts AF. Problems associated with the theoretical analysis of the burning of wood. 13th Symp (Int) Comb 1971:893–903.
[50] Haseli Y, van Oijen JA, de Goey LPH. Modeling biomass particle pyrolysis with temperature-dependent heat of reactions. J Anal Appl Pyrol 2011;90:140–54.
[51] Antal MJ, Grønli M. The art, science, and technology of charcoal production. Ind Eng Chem Res 2003;42:1619–40.
[52] Xu X, Matsumura Y, Stenberg J, Antal MJ. Carbon-catalyzed gasification of organic feedstocks in supercritical water. Ind Eng Chem Res 1996;35:2522.
[53] Brandt P, Larsen E, Henriksen U. High tar reduction in a two-stage gasifier. Energy Fuels 2000;14:816.
[54] Hajaligol MR, Howard JB, Peters WA. An experimental and modeling study of pressure effects on tar release by rapid pyrolysis of cellulose sheets in a screen heater. Combust Flame 1993;95:47.
[55] Wang L, Skreiberg O, Gronli M, Specht G, Antal Jr MJ. Is elevated pressure required to achieve a high fixed-carbon yield of charcoal from biomass? 2. The importance of particle size. Energy Fuels 2013;27:2146–56.
[56] Wang L, Trninic M, Skreiberg O, Gronli M, Considine R, Antal MJ. Is elevated pressure required to achieve a high fixed-carbon yield of charcoal from biomass? 1. Round robin results for three different corncob materials. Energy Fuels 2011;25:3251–65.